Influence of the ^{6,7}Li breakup process on the near barrier elastic scattering by heavy nuclei

A. M. M. Maciel, P. R. S. Gomes, J. Lubian,* R. M. Anjos, R. Cabezas, G. M. Santos, C. Muri, and S. B. Moraes
Instituto de Física, Universidade Federal Fluminense, Av. Litorânea s/n, Gragoatá, Niterói, R.J., 24210-340, Brazil

R. Liguori Neto, N. Added, and N. Carlin Filho
Instituto de Física, Universidade de São Paulo, C.P. 20516, São Paulo, 01498-970, Brazil

C. Tenreiro
Departamento de Física, Facultad de Ciencias, Universidad de Chile, Casilla 653, Santiago, Chile
(Received 29 October 1998)

Angular distributions of the elastic scattering of the ^{6,7}Li on ^{138}Ba were measured, in the energy range $21 \leqslant E_{\mathrm{lab}} \leqslant 32$ MeV. The analysis of the data was performed via the optical model, using the Woods-Saxon potential, in order to find the energy dependence of the real and imaginary parts of the nuclear potential. The existence of a threshold anomaly for the ^{7}Li scattering and its absence for the ^{6}Li one was observed. It is interpreted that the breakup of ^{6}Li, with dissociation energy smaller that its first excited state, is responsible for the vanishing of the threshold anomaly. [S0556-2813(99)01404-1]

PACS number(s): 25.70.Mn, 24.10.Eq, 25.60.Gc

I. INTRODUCTION

The existence of the threshold anomaly in the interacting potential for the elastic scattering has been found for many systems (see, for instance, Refs. [1,2] and references therein). This anomaly shows up as a localized peak in the real part of the interacting potential (usually assumed as an optical potential or doubled folding potential) in the neighborhood of the Coulomb barrier and it is associated with the decrease of the imaginary part of the interacting potential in the same energy region. It has been shown that this correlation between the real and imaginary parts of the interacting potential is due to causality and consequently that they obey the dispersion relations [3].

For instance, coupled channel calculations carried out for the system ^{16}O+^{208}Pb [4] have shown that the behavior of the optical potential can be explained by taking into account the inelastic and transfer channels, typically surface reactions, in the coupling scheme. This anomaly in the behavior of the reaction potential due to the closure of the direct surface reaction channels, at energies near the Coulomb barrier, leads to the enhancement of the fusion cross section [3,5].

A subject of increasing interest in recent years is the investigation of the effect of the breakup channel on the other reaction channels when weakly bound projectiles, like ^{6,7}Li, impinge on heavy targets. ^{6}Li and ^{7}Li have similar structures and show almost the same behavior at high energies, but their differences become evident at low energies. ^{6}Li has a threshold breakup $(\alpha+d)$ of 1.48 MeV, smaller than the dissociation energy of the ^{7}Li$(\alpha+t)$, 2.45 MeV. The ^{6}Li nucleus does not have excited states strongly coupled to the ground state (its first excited state is 2.185 MeV), and it is spherical in its ground state, whereas the ^{7}Li nucleus is deformed in its ground state and its first excited state (0.477 61 MeV) is strongly coupled to the ground state. The excitation of this state should produce an attractive polarization potential. As a result of the characteristics of these projectiles, it was suggested [6] that their dissociations should influence the behavior of the real part of the optical potential at energies near the Coulomb barrier, leading to the absence of the threshold anomaly. This effect could be interpreted as an inhibition of the fusion process by the breakup of the projectile, as predicted [7,8] and measured for the light systems [9]. The small separation energies for the ^{6}Li and ^{7}Li favors the breakup process, but the consequence of that on the fusion and elastic scattering cross sections is not yet clear. The understanding of the role of the breakup on the reaction mechanisms, for these projectiles, is also quite important, as a reference for studies with ^{11}Li projectiles.

Keeley and co-workers [10] analyzed the elastic scattering of ^{6,7}Li on ^{208}Pb at energies near the Coulomb barrier. They have found the absence of the threshold anomaly of the interacting potential for the ^{6}Li projectile and its presence for the ^{7}Li projectile. In their work they used a double-folded potential for the real part of the interacting potential and the Woods-Saxon potential for the imaginary part. Further experimental investigation on this subject, with other systems, is required in order to confirm this effect.

In the present work, we analyze the elastic scattering of ^{6,7}Li on ^{138}Ba at near-barrier energies. The ^{138}Ba is a spherical neutron magic nucleus and it is expected that the collective excitations of the target, vibrational like, do not play an important role for these reactions.

Section II of this paper is devoted to describing the experiment. In Sec. III we present the results of the optical model calculations, and finally, in Sec. IV, some conclusions are drawn.

II. EXPERIMENTAL DETAILS

The experiments were performed at the 8UD Pelletron accelerator of the University of São Paulo. The ^{6,7}Li beams

*Permanent address: Center of Applied Studies to Nuclear Development, P.O. Box 6122, Havana, Cuba.

were extracted from a natural lithium sample, mixed with silver, and placed at a SNICS source. The beam intensities on the targets were typically of the order of 10 nA for ^{6}Li and 100 nA for ^{7}Li. The beam energies were within the range from 21 to 32 MeV for ^{7}Li and from 21 to 28 MeV for ^{6}Li, corresponding to energies just below the nominal Coulomb barrier to 50% above this value ($V_{b\mathrm{lab}} \approx 22$ MeV). The maximum energy was limited by the detector thicknesses. The ^{138}Ba targets were made by the evaporation of enriched $BaCO_3$ on 15 μg/cm^2 carbon backings. Their thicknesses were of the order of 100–200 μg/cm^2. Some ^{12}C and ^{16}O contaminations were detected and they were used in the energy calibration of the spectra. Four targets were mounted at the center of a 1 m diameter scattering chamber.

The detection system was an array containing nine silicon surface barrier detectors, placed at 40 cm from the target. The detector thicknesses were 150 μm. The angular separation between two adjacent detectors was 5°. In front of each detector there was a set of collimators and circular slits for the definition of solid angles and to avoid slit-scattered particles. The angle determination was made by reading on a goniometer with a precision of 0.5°. A monitor was placed at 30° with the beam direction. The energy resolutions of the detectors were of the order of 300–500 keV [full width at half maximum (FWHM)], good enough to separate the elastic peak from the inelastic scattering to the first excited state of ^{138}Ba and of Li isotopes peaks. The angular distribution data were taken in the range $25° \leqslant \theta_{\mathrm{lab}} \leqslant 135°$. The relative solid angles of the detectors were determined by the Rutherford scattering of lithium isotopes on the ^{138}Ba target, at the same angle.

The uncertainties in the differential cross section data vary from 1% to 10% for the elastic scattering. The inelastic scattering was not analyzed in this work, due to its very low statistic.

III. ELASTIC SCATTERING ANALYSIS

For the theoretical description of the experimental angular distributions, the optical model was used, considering an optical potential in the form

$$V(r) = -V_0 f(r,R_v,a_v) - iW_{0V} f(r,R_w,a_w) + V_{\mathrm{Coul}}, \quad (1)$$

where

$$f(r,R_i,a_i) = \frac{1}{1+\exp[(r-R_i)/a_i]},$$

$$R_i = r_i(A_p^{1/3} + A_t^{1/3}), \quad i = v,w.$$

V_0 and W_{0V} are the real and volume imaginary strengths and r_i and a_i their reduced radii and diffusenesses, respectively. $f(r,R_i,a_i)$ is the form factor of the Woods-Saxon potential and V_{Coul} is the Coulomb potential of a uniform charged sphere with radius $R_C = 1.22(A_p^{1/3} + A_t^{1/3})$. A_p and A_t are the projectile and target mass, respectively.

All the calculations were performed using the ECIS code [11]. As a starting point in the determination the optical potential parameters, a χ^2-fit procedure was carried out, adjusting the radii and diffusenesses at the highest of energies, where nuclear effects are expected to be more significant.

TABLE I. Sets of optical model parameters that equally well fit the experimental data, at different diffusenesses for the ^{6}Li + ^{138}Ba system.

E_{lab} [MeV]	21	22	23	24	26	28
			$a_v = a_w = a_s = 0.55$ fm			
V_0 [MeV]	120.16	83.03	99.38	85.23	81.64	71.99
W_{0V} [MeV]	0.40	0.40	3.67	8.69	0.78	2.94
W_{0S} [MeV]	80.16	27.77	30.15	23.63	12.51	5.11
			$a_v = a_w = a_s = 0.65$ fm			
V_0 [MeV]	27.65	28.64	31.17	28.55	31.33	32.17
W_{0V} [MeV]	0.29	0.43	1.78	2.93	2.74	1.66
W_{0S} [MeV]	28.60	11.74	13.84	11.63	7.84	6.45
			$a_v = a_w = a_s = 0.75$ fm			
V_0 [MeV]	10.41	14.86	13.26	12.77	14.88	14.65
W_{0V} [MeV]	0.20	0.53	1.92	3.08	4.66	3.35
W_{0S} [MeV]	12.71	5.77	7.27	6.33	4.93	4.85

Any attempt to fit the experimental data has failed. These results showed the need for the inclusion of a surface imaginary part W_S of derivative form:

$$W_S(r) = -4iW_{0S}\frac{d}{dr} f(r,R_s,a_s). \quad (2)$$

The presence of the surface imaginary potential indicates that some direct reaction processes, like inelastic scattering, transfer, or breakup (with surface form factor), could play an important role in the reaction process for these systems.

With the inclusion of the surface potential, a new fit procedure was carried out, assuming the radius of the real and surface parts of the optical potential to be equal. Then, these values were fixed as $r_v = r_s = 1.239$ fm, $r_w = 1.14$ fm for the ^{6}Li+^{138}Ba system and $r_v = r_s = 1.237$ fm, $r_w = 1.14$ fm for the ^{7}Li+^{138}Ba system.

Using these radii we tried to find some families of optical potential parameters that equally well describe the angular distributions. The details of these procedures can be found in Refs. [5,12,13]. Considering the diffusenesses $a_v = a_w = a_s$, and varying them within the interval from 0.50 fm to 0.80 fm, in steps of 0.05 fm, the values of the potential strength were derived. Tables I and II show some of these optical potential parameter sets for the ^{6}Li+^{138}Ba and ^{7}Li+^{138}Ba systems, respectively, for different energies and some diffuseness values. These sets describe equally well the angular distributions; i.e., they give similar χ^2 values. For some diffusenesses, more than one set of potential strengths described almost the same way the experimental angular distributions. In order to remove this ambiguity, the well-known linear behavior of the reaction cross section with the inverse of energy for energies above the Coulomb barrier was used to fix the optical potential parameters.

The objective of this procedure is to reduce the ambiguities of the optical potential parameters by finding the so-called *radius of sensitivity* [5,12,13], in order to find the energy dependence of the optical potential at this radius. It corresponds to the radius where potentials, giving comparable fits to the data, have the same value.

TABLE II. Sets of optical model parameters that equally well fit the experimental data, at different diffusenesses for the ^{7}Li+^{138}Ba system.

E_{lab} [MeV]	21	22	23	24	28	30	32
			$a_v=a_w=a_s=0.55$ fm				
V_0 [MeV]	115.63	74.58	66.77	71.69	50.28	54.16	46.10
W_{0V} [MeV]	0.20	5.80	11.34	0.28	32.09	20.32	7.69
W_{0S} [MeV]	3.78	14.91	8.78	10.66	0.26	0.50	0.48
			$a_v=a_w=a_s=0.65$ fm				
V_0 [MeV]	50.05	30.81	28.18	28.07	24.09	26.66	24.85
W_{0V} [MeV]	0.20	3.00	10.16	3.09	37.57	38.00	37.74
W_{0S} [MeV]	2.05	6.52	4.29	6.50	0.32	0.50	0.30
			$a_v=a_w=a_s=0.75$ fm				
V_0 [MeV]	26.91	17.62	15.98	13.82	13.32	14.49	13.88
W_{0V} [MeV]	0.20	2.80	10.05	5.05	27.34	29.32	31.27
W_{0S} [MeV]	1.42	3.19	1.98	3.81	0.25	0.50	0.30

From Tables I and II, one can notice the high sensibility of the potential strengths to the changes of the diffusenesses. The reason for this dependence is evident: to obtain the same value of the real and imaginary parts of the potential at the *radius of sensitivity*, one has to have deeper potential if their diffusenesses are smaller and *vice versa*. Another feature of the potential sets of Tables I and II is a general trend to increase the volume imaginary part of the optical potential and to decrease the surface imaginary potential as the energy grows. This is in agreement with the prescriptions of the optical model. The increase of the volume part of the optical potential corresponds to the growth of the fusion cross section as the energy increases at near barrier energies. The decrease of the surface part of the optical potential indicates the importance of the surface excitations, like inelastic scattering, transfer and nuclear breakup, at near-barrier energies, and the lack of importance of these channels at higher energies. From Tables I and II one can see that the energy dependence of the real part of the potential is smooth, when compared with the imaginary parts.

Figures 1 and 2 show the angular distributions of elastic scattering for the ^{6}Li+^{138}Ba and ^{7}Li+^{138}Ba, respectively, calculated with any of the sets of parameters of Tables I and II (solid lines).

With the values of the potential strengths obtained at each energy for every value of the diffuseness, we obtained a *radius of sensitivity* as a point of intersection of these potentials (see for details Refs. [5,12,13]). Once we had the *radius of sensitivity* at each energy for the real and total imaginary parts (the sum of volume and surface parts) of the interacting potential, we derived their mean values as 12.15 fm and 11.27 fm for the ^{6}Li+^{138}Ba and ^{7}Li+^{138}Ba systems, respectively.

In Figs. 3 and 4, the energy dependence of the potentials at these radii for both systems is shown. The points represent the values of the real and imaginary potentials, evaluated at the *radius of sensitivity* for each system. The error bars represent the range of deviation of the potential, corresponding to distinct sets of parameters with different values of diffusenesses and roughly the same χ^2. The solid lines represent the results of the calculations using the dispersion relations [1].

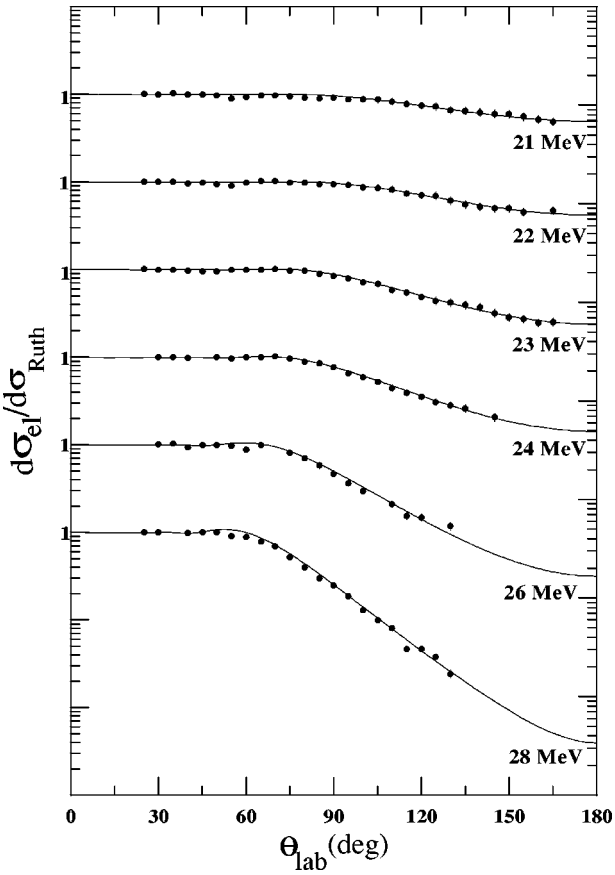

FIG. 1. Elastic scattering differential cross section for the system ^{6}Li+^{138}Ba at different bombarding energies. The experimental error bars are smaller than the points. The solid line corresponds to the optical model calculation using one of the sets of Table I.

From Fig. 3 a rather smooth energy dependence of the real and imaginary parts of the optical potential can be seen, except for the lower one, $E=21$ MeV, measured at subbarrier Coulomb energy. This indicates that no optical potential anomaly is present near the Coulomb barrier for the system ^{6}Li+^{138}Ba. The opposite situation occurs with the system ^{7}Li+^{138}Ba. From Fig. 4 one can see an anomalous energy dependence of both potentials at the lowest energies, near the energy corresponding to the Coulomb barrier. The imaginary optical potential increases rapidly at near-barrier energies and then drops slowly. This, according to the dispersion relations [1], leads to a real potential shown in the upper part of Fig. 4. The decrease of the imaginary potential at high energies is forced by the values of the real potential at 28, 30, and 32 MeV. However, if one imposes a constant value for the imaginary potential for energies above the Coulomb barrier, which is allowed by the size of the error bars, the threshold anomaly is still present, and only the fit of the real potential is slightly affected.

The results of the analysis show important differences in the elastic scattering of the two lithium isotopes. Of course, as one has the same target for both systems, one should expect that the difference between their elastic scattering should not be governed by the inelastic excitations of the target, but by the structural characteristics of the projectiles.

The presence of the anomaly for the ^{7}Li elastic scattering can be interpreted as the effect of the strong couplings with

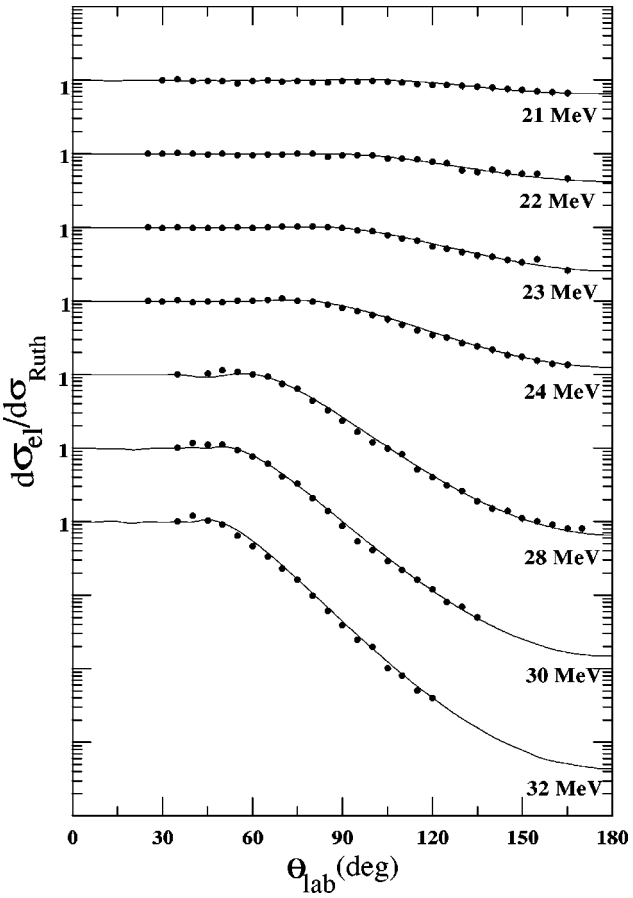

FIG. 2. Elastic scattering differential cross section for the system ^{7}Li+^{138}Ba at different bombarding energies. The experimental error bars are smaller than the points. The solid line corresponds to the optical model calculation using one of the sets of Table II.

the first excited state of the ^{7}Li inelastic channel, the one-neutron transfer and other reaction channels at near barrier energies, leading to an attractive polarization potential. Consequently, it may also be interpreted as a signature of the fusion cross section enhancement. One should remember that the dissociation energy of ^{7}Li into ^{4}He+^{3}H is around 2.45 MeV, much higher than the energy of its first excited

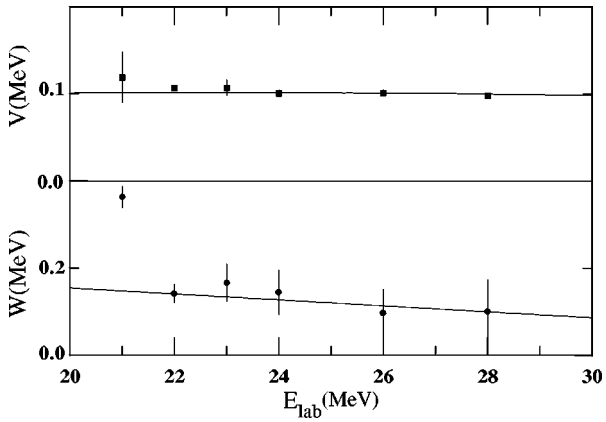

FIG. 3. Values of the real and imaginary parts of the optical potential at the *radius of sensitivity*, equal to 12.15 fm, for the system ^{6}Li+^{138}Ba. The solid line corresponds to the dispersion relation calculations.

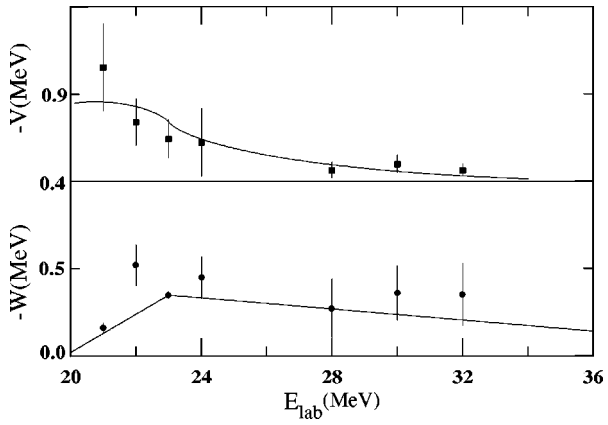

FIG. 4. Values of the real and imaginary parts of the optical potential at the *radius of sensitivity*, equal to 11.27 fm, for the system ^{7}Li+^{138}Ba. The solid line corresponds to the dispersion relation calculations.

state, 0.478 MeV. Consequently, there is a high probability of exciting the first excited state of ^{7}Li. Recently, Keeley and Rusek [14] have shown that the potential anomaly at near-barrier energies for the ^{7}Li+^{208}Pb is mostly governed by the one-neutron transfer channel. The situation could be the same for the system studied in the present work.

The absence of the anomaly for the very weakly bound ^{6}Li induced elastic scattering is a signature that, for this projectile, the breakup is the dominant direct channel, leading to weak coupling between the elastic and inelastic channels. Unlike the ^{7}Li, the dissociation energy of ^{6}Li into ^{4}He+^{2}H is around 1.5 MeV, much smaller than the energy of its first excited state (2.185 MeV), and consequently the probability of exciting this state is very low. The coupling to the breakup channel may contribute as a repulsive effective polarization potential, which may exceed the attractive term arising from the inelastic coupling to bound states or to be of the same order as that. Therefore, for very weakly bound nuclei, such as ^{6}Li, this effect may be strong enough to affect the real part of the optical potential near the Coulomb barrier in such way that it leads to the absence of the threshold anomaly in the scattering of these projectiles. The need for the imaginary surface potential for describing the elastic scattering of ^{6}Li on ^{138}Ba is a signature that nuclear interactions might play an important role in the dissociation of the ^{6}Li projectile. Therefore, it seems reasonable to expect that the fusion, at low energies, should be enhanced for ^{7}Li relative to ^{6}Li, whereas quasielastic reactions should be stronger for the ^{6}Li and dominated by the breakup.

These conclusions strengthen the ones drawn by Keeley and co-workers [10] for the ^{6,7}Li+^{208}Pb systems.

If this interpretation is correct, the total reaction cross sections should be higher for the ^{6}Li+^{138}Ba system, due to its stronger surface imaginary potential (see Tables I and II). Figure 5 shows the reaction cross sections for both systems. The points are the mean values, obtained by averaging the reaction cross section derived for different sets of parameters, at each energy. Although they are similar at high energies, one can notice that the reaction cross section at low energies is indeed larger for the ^{6}Li+^{138}Ba system.

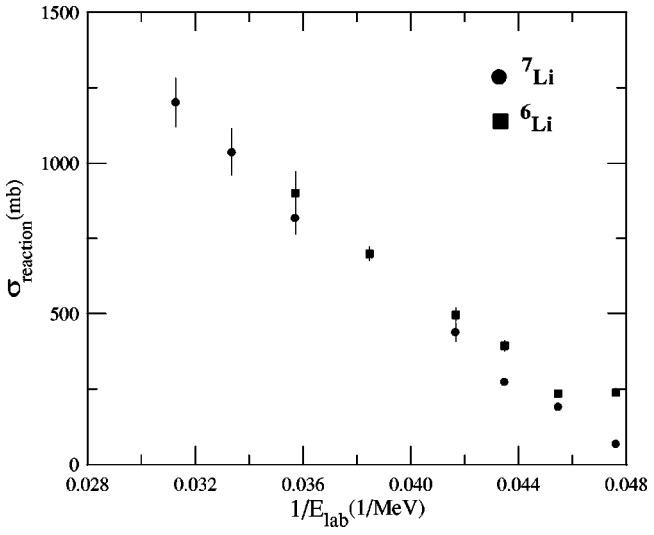

FIG. 5. Rection cross section for the system ^{6,7}Li+^{138}Ba versus the inverse of the energy.

IV. SUMMARY

In this paper original data for the elastic scattering angular distributions for the ^{6,7}Li+^{138}Ba systems at sub- and near-barrier energies are presented, with the aim of investigating the role of the breakup channel on reactions and elastic processes, with heavy targets. This was done by the study of the energy dependence of the optical potential at the *radius of sensitivity*.

The results of the optical model analysis show important differences in the elastic scattering of the two lithium isotopes. For the optical potential that describes the elastic scattering of ^{7}Li on ^{138}Ba, the well-known threshold anomaly is observed, while for the elastic scattering of ^{6}Li on ^{138}Ba the anomaly is no longer present. Its presence for the ^{7}Li elastic scattering can be interpreted as the effect of the strong couplings with the first excited state of the ^{7}Li inelastic channel, the one-neutron transfer, and any other direct reaction channels at near barrier energies, leading to an attractive polarization potential. The absence of the threshold anomaly for the ^{6}Li induced scattering is an evidence that, for this projectile, the breakup is the dominant direct channel, leading to weak coupling between the elastic and inelastic or transfer channels. Moreover, the breakup channel should produce a repulsive polarization potential that compensates the attractive potential produced by other direct channels.

From the present study, it is expected that fusion, at low energies, should be enhanced for ^{7}Li relative to ^{6}Li, whereas quasielastic reactions should be stronger for ^{6}Li and dominated by the breakup. It will be interesting to measure the fusion cross section for these systems, in order to test this conclusion.

ACKNOWLEDGMENTS

The authors would like to thank the Conselho Nacional de Desenvolvimento Científico e Tecnlógico (CNPq), Fundação de Amparo à Pesquisa do Estado do Rio de Janeiro (FAPERJ), Centro Latinoamericano de Física (CLAF), and Coordenação de Aperfeiçoamento de Pessoal de Nível Superior (CAPES) for financial support.

[1] G. R. Satchler, Phys. Rep. **199**, 147 (1991).
[2] B. R. Fulton, in *Heavy Ion Collisions at Energies Near the Coulomb Barrier*, edited by M. A. Nagarajan, Int. Phys. Conf. Ser. No. 110 (IOP, Bristol, 1991), Sec. I, p. 15.
[3] M. A. Nagarajan, C. C. Mahaux, and G. R. Satchler, Phys. Rev. Lett. **54**, 1136 (1985).
[4] I. J. Thompson, M. A. Nagarajan, J. S. Lilley, and M. J. Smithson, Nucl. Phys. **A505**, 84 (1989).
[5] C. Muri, R. M. Anjos, R. Cabezas, P. R. S. Gomes, S. B. Moraes, A. M. M. Maciel, G. M. Santos, J. Lubian, M. M. Sant'Anna, C. Tenreiro, R. Liguori Neto, J. C. Acquadro, and P. A. B. Freitas, Eur. Phys. J. A **1**, 143 (1998).
[6] C. Mahaux, H. Ngo, and G. R. Satchler, Nucl. Phys. **A449**, 354 (1986).
[7] L. F. Canto, R. Donangelo, M. S. Hussein, and M. P. Pato, Nucl. Phys. **A542**, 131 (1992).
[8] M. S. Figueira, E. M. Szanto, A. Szanto de Toledo, M. P. Pato, M. S. Hussein, and L. F. Canto, Phys. Rev. C **46**, 1139 (1992).
[9] J. Takahashi, M. Munhoz, E. M. Szanto, N. Carlin, N. Added, A. A. P. Suaide, M. M. de Moura, R. Liguori Neto, A. Szanto de Toledo, and L. F. Canto, Phys. Rev. Lett. **78**, 30 (1997).
[10] N. Keeley, S. J. Bennet, N. M. Clarke, B. R. Fulton, G. Tungate, Nucl. Phys. **A571**, 326 (1994).
[11] J. Raynal, in *Workshop on Applied Nuclear Theory and Model Calculations for Nuclear Technology Aplications*, Trieste, 1988, edited by M. K. Mehta and J. J. Schmid (World Scientific, Singapore, 1989), pp. 506–536.
[12] M. E. Brandan, J. R. Alfaro, A. Menchaca-Rocha, J. Gomez del Campo, G. R. Satchler, P. H. Stelson, H. J. Kim, and D. Shapira, Phys. Rev. C **48**, 1147 (1993).
[13] A. Zerwekh, R. Liguori Neto, N. Added, J. C. Acquadro, N. Carlin Filho, M. Frizzarini, F. Malandrino, J. Lubian, R. Cabezas, P. R. S. Gomes, R. M. Anjos, G. M. Santos, A. M. M. Maciel, C. Muri, S. B. Moraes, G. Ramirez, and C. Tenreiro, Phys. Rev. C **58**, 3445 (1998).
[14] N. Keeley and K. Rusek, Phys. Rev. C **56**, 3421 (1997).